AIP | Review of Scientific Instruments

Data acquisition in a high-speed rotating frame for New Mexico Institute of Mining and Technology liquid sodium αω dynamo experiment

Jiahe Si, Stirling A. Colgate, Hui Li, Joe Martinic, and David Westpfahl

Citation: Rev. Sci. Instrum. **84**, 104501 (2013); doi: 10.1063/1.4825354
View online: http://dx.doi.org/10.1063/1.4825354
View Table of Contents: http://rsi.aip.org/resource/1/RSINAK/v84/i10
Published by the AIP Publishing LLC.

REVIEW OF SCIENTIFIC INSTRUMENTS **84**, 104501 (2013)

Data acquisition in a high-speed rotating frame for New Mexico Institute of Mining and Technology liquid sodium $\alpha\omega$ dynamo experiment

Jiahe Si,[1,a)] Stirling A. Colgate,[2] Hui Li,[2] Joe Martinic,[1] and David Westpfahl[1]
[1]*New Mexico Institute of Mining and Technology, Socorro, New Mexico 87801, USA*
[2]*Los Alamos National Laboratory, Los Alamos, New Mexico 87544, USA*

(Received 5 August 2013; accepted 2 October 2013; published online 22 October 2013)

New Mexico Institute of Mining and Technology liquid sodium $\alpha\omega$-dynamo experiment models the magnetic field generation in the universe as discussed in detail by Colgate, Li, and Pariev [Phys. Plasmas **8**, 2425 (2001)]. To obtain a quasi-laminar flow with magnetic Reynolds number $R_m \sim 120$, the dynamo experiment consists of two co-axial cylinders of 30.5 cm and 61 cm in diameter spinning up to 70 Hz and 17.5 Hz, respectively. During the experiment, the temperature of the cylinders must be maintained to 110 °C to ensure that the sodium remains fluid. This presents a challenge to implement a data acquisition (DAQ) system in such high temperature, high-speed rotating frame, in which the sensors (including 18 Hall sensors, 5 pressure sensors, and 5 temperature sensors, etc.) are under the centrifugal acceleration up to 376g. In addition, the data must be transmitted and stored in a computer 100 ft away for safety. The analog signals are digitized, converted to serial signals by an analog-to-digital converter and a field-programmable gate array. Power is provided through brush/ring sets. The serial signals are sent through ring/shoe sets capacitively, then reshaped with cross-talk noises removed. A microcontroller-based interface circuit is used to decode the serial signals and communicate with the data acquisition computer. The DAQ accommodates pressure up to 1000 psi, temperature up to more than 130 °C, and magnetic field up to 1000 G. First physics results have been analyzed and published. The next stage of the $\alpha\omega$-dynamo experiment includes the DAQ system upgrade. [http://dx.doi.org/10.1063/1.4825354]

I. INTRODUCTION

A. The NMIMT liquid sodium $\alpha\omega$-dynamo experiment

Magnetic fields are believed to hold the key to understanding many phenomena in the universe. For many astrophysical systems, it is generally assumed that magnetic fields are amplified from very weak seed fields by the interaction of electrically conducting fluid motion, the so-called dynamo mechanism.[2] Since the dynamo mechanism was first proposed by Sir Joseph Larmor[3] in 1919, there is not yet a widely accepted theory and understanding of how exactly the dynamo process works. One of the reasons is that only a limited amount of experimental work has been carried out due to the major experimental limitations involved.

A candidate for dynamo mechanism, the $\alpha\omega$-dynamo, can be idealized as

$$B_{poloidal} \xrightarrow{\omega\text{-effect}} B_{toroidal} \xrightarrow{\alpha\text{-effect}} B_{poloidal}.$$

The original suggestion of Parker[4] was that the differential rotation within an astrophysical system (such as a star or a galaxy) can create a relatively large shear gain by winding up a small radial flux (poloidal), necessary for the ω-gain(G_ω). Furthermore, Parker[4] suggested that a fraction of the amplified toroidal flux must be converted to poloidal flux by means of cyclonic motion. But Moffat[2] observed that a cyclone makes many revolutions before damping and, therefore, would average the poloidal flux rather than add linearly to the original. Turbulence is frequently invoked to create a statistical source of helicity[5] (the α-effect of the stretch-twist-fold deformations). Although there are experiments[6] to explore the possibility of amplifying a seed magnetic field through the generation of turbulent electromotive forces (EMF),[2] this has yet to be demonstrated experimentally.

The key difference between the New Mexico Institute of Mining and Technology (NMIMT) liquid sodium $\alpha\omega$-dynamo experiment and other dynamo experiments is the recognition that two simple driven *coherent flows* can make a *coherent $\alpha\omega$* dynamo.

In our view the fluid flow must be primarily coherent as opposed to statistically incoherent or random, which is also the primary conclusion of Tobias and Cattaneo.[7] For accretion disks around supermassive black holes, plumes driven by star-disk collisions are a unique solution to the generation of helicity and can lead to an efficient dynamo.[1,8,9] This is because plumes damp in less than a revolution by entrainment of surrounding fluid and furthermore rotate in the same direction by the same fraction every time due to the competition between entrainment and conservation of the original angular momentum. Through this α-deformation, a portion of the enhanced toroidal flux can be converted to poloidal flux.

In order to demonstrate an astrophysical dynamo experimentally, at least $1/G_\omega$ of the enhanced toroidal flux must be converted to poloidal flux. Therefore, the higher the gain obtained during ω-deformation, the easier it is to achieve the dynamo. This relatively high ω-gain is obtained with high Reynolds number, quasi-laminar (low turbulent), nearly stable Couette flow, as shown in Fig. 1(a). This flow pattern is

a)Electronic mail: jsi@nmt.edu.

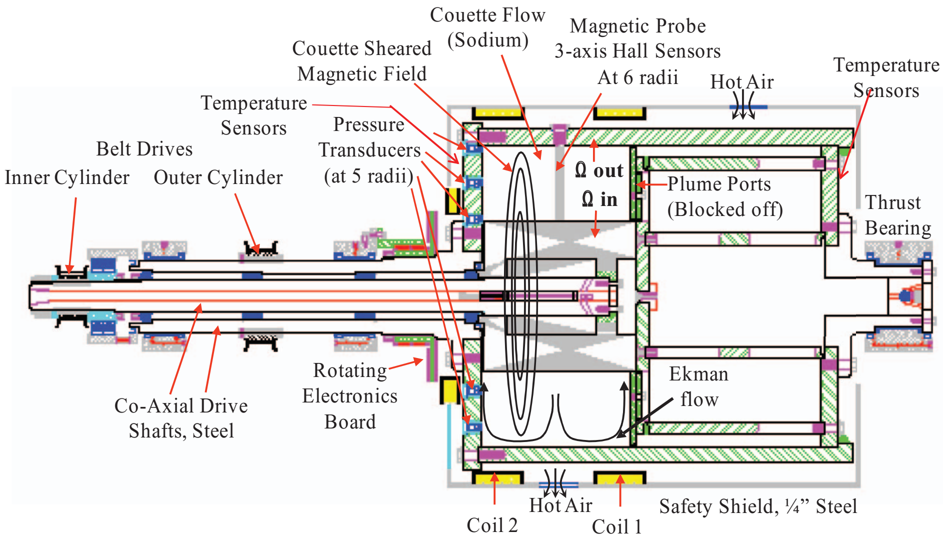

(a) the dynamo apparatus: the ω-phase

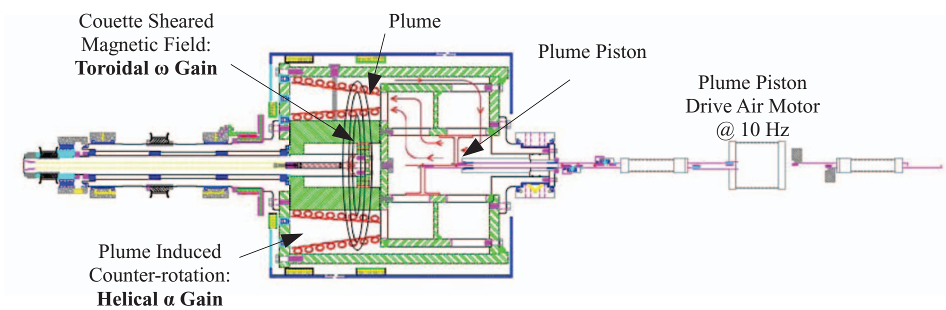

(b) the dynamo apparatus: the α-phase

FIG. 1. Dynamo apparatus: The outer cylinder is 61 cm in diameter, the inner 30.5 cm. (a) The ω-phase. The outer cylinder is separated into two parts by a plate in the middle. The right part is reserved for future α phase. The left part is an annulus where a near-stable Couette flow is generated. At full speed $\Omega_{out} = 2\pi \times 17.5$ rad/s and $\Omega_{in} = 2\pi \times 70$ rad/s, the Reynolds number Re is $\sim 1.3 \times 10^7$ and magnetic Reynolds number Rm ~ 120. Pressure sensors are mounted on the left end-plate at 5 radii; 2 temperature sensors are on each end-plate; a magnetic probe with 18 Hall sensors in 3 orthogonal directions is in the mid-plane of the annulus. A rotating electronics board is mounted on the left just outside the safety shield to collect data from the sensors. (b) The α-phase. Plumes are developed into the annulus on the left by a proposed air-motor-driven piston. A set of plumes every 6 turns is a likely threshold for positive gain.

similar to what is expected in a Keplerian accretion disk around a central massive black hole. In our dynamo experiment, the Couette flow is generated between two co-axial cylinders of 30.5 and 61 cm in diameter spinning up to 70 and 17.5 revolution per second, or 4200 and 1050 rpm, respectively (the 4:1 rotation ratio is the limiting stable Couette flow ratio for a radius ratio of 2:1[10]). This configuration gives us the maximal magnetic Reynolds number for the rotational Couette flow of

$$\mathrm{Rm}_\omega = \frac{\Omega_{out} R_{out}(R_{out} - R_{in})}{\eta} \sim 120,$$

with the magnetic diffusivity of liquid sodium $\eta = 820\,\mathrm{cm}^2/\mathrm{s}$ at 110 °C. And given the kinematic viscosity coefficient of liquid sodium $\nu = 7.1 \times 10^{-3}\,\mathrm{cm}^2/\mathrm{s}$, the maximal Reynolds number of the Couette flow of our experiment is

$$\mathrm{Re}_\omega = \frac{\Omega_{out} R_{out}(R_{out} - R_{in})}{\nu} \sim 1.3 \times 10^7.$$

An orthogonal flow system is being implemented for the α-deformation, as shown in Fig. 1(b). This is implemented with driven plumes, parallel to the axis, analogous to convection plumes in stars or planets, or plumes produced by star-disk collisions in accretion disks. The α-deformation converts a fraction of the enhanced toroidal field, produced by the differential rotation, back into the "seed" poloidal field by the rotation of the plume around the axis of buoyancy deformation. The necessary coherence is the phase relationship between the axial displacement of the plume flow and the subsequent rotation about its own axis by its radial expansion and conservation of angular momentum. Experimental confirmation of this flow configuration has been demonstrated in water experiments.[11,12]

B. The experimental challenge of data acquisition

Obtaining valuable data from the apparatus poses a real challenge due to the nature of the experimental setup. The majority of experiments on circular Couette flows are performed with the outer cylinder held stationary. Since $\partial(\Omega r^2)/\partial r < 0$, such setups are unstable with ideal inviscid flows. A few experiments[13,14] can be operated in the linearly stable regime with $\Omega_{out} \geq \frac{R_{in}^2}{R_{out}^2}\Omega_{in} > 0$. To the best of our knowledge, there is no other experiment which reaches Re $\sim 10^7$. None has data acquisition (DAQ) in such a high-g, high-temperature rotating frame with many sensors.

At full speed, the centrifugal acceleration at the outer cylinder is up to 376g, a near limiting value for the rotating electronics held in sockets. The temperature of the cylinders must be maintained no lower than 110 °C to ensure that the sodium remains fluid. In many hydrodynamic experiments (e.g., with water or oils) the flows can be visualized and measured by a wide variety of techniques. However, it is nontrivial to make measurements in liquid sodium. To measure the changing magnetic field, as shown in Fig. 1(a), a magnetic probe with 18 Hall sensors in 3 orthogonal directions and 6 radial positions is used to obtain magnetic data in the mid-plane of Couette annulus. There are 5 pressure sensors on the left end-plate to measure the pressure profile. On each end-plate, 2 temperature sensors monitor the liquid sodium temperature, plus one on the circuit board to monitor the electronic component temperature. All signals from the sensors must be digitized and transmitted reliably from the rotating frame of the outer cylinder.

In this paper, we describe the design of the data acquisition system in Sec. II, the results in Sec. III, and the conclusion and future plan in Sec. IV.

Although the DAQ system is designed specifically for the NMIMT $\alpha\omega$-dynamo experiment, similar systems may be used in experiments requiring data acquisition from rotating frames.

II. SYSTEM DESCRIPTION

A. Overview

The electrical power for the rotating, diagnostic system is provided through 2 sets of carbon brushes and slip rings. Because the electrical continuity of carbon brushes and slip rings is notoriously intermittent and noisy, the analog signals are digitized, converted to serial signals by an analog-to-digital converter (ADC) and field-programmable gate array (FPGA) programmable logic in the rotating frame. The digital signals are sent through ring/shoe sets capacitively (∼50 pf) with a clearance of 0.02 cm between shoe and ring. The serial signal is then reshaped with cross-talk noises removed, then converted to/from differential signals. One hundred feet away, a microcontroller-based interface circuit is used to decode the signals and communicate with the data acquisition computer through Universal Serial Bus (USB) connection.

As shown in Fig. 2, the data acquisition is implemented through 5 function blocks: a Linux based data acquisition computer, a USB microcontroller (Microchip® 18F4550) interface, a "stationary board," a trolley/rings set, and a "rotating board."

The following is a typical workflow:

1. The data acquisition computer specifies which sensors are needed for different experimental requirements, and then sends a sensor list to the USB interface.
2. The USB microcontroller interface receives the sensor list, stores it. Then the interface sends differential serial address signals of the corresponding sensors one by one to the stationary board in a fixed interval of 100 μs through BNC cables. After the interface sends a serial address signal, it waits for the serial data signal.
3. The serial differential address signal is converted to transistor-transistor logic (TTL) address signal by the line receiver on the stationary board.
4. The serial address signal is coupled through the shoe and slip ring set capacitively.
5. The serial address signal is reshaped by the Address In Driver (AID), and then sent to a programmed FPGA (Altera® EMP7128LC84-6).
6. The FPGA receives the serial address signal, decodes it, and converts to address control signals for multiplexers on the rotating board to select the analog signal from the corresponding sensors. The analog signal is digitized by an 8-bit analog-to-digital converter (Maxim® MAX118) and sent back to the FPGA. The FPGA receives the parallel data signal and converts it to serial data signal and sends the data signal to the slip ring.
7. The serial data signal is coupled through the slip ring and shoe set capacitively.
8. The serial data signal is reshaped by the Data Out Driver (DOD), and then sent to the stationary board.
9. The serial TTL data signal is converted to differential data signal by the line driver on the stationary board.
10. The USB microcontroller interface receives the serial data signal, converts, and stores it in a buffer for USB communication. If it does not receive serial data signal back in 100 μs (due to reasons such as the rotating board is not on, transmission cables are broken, or something is wrong on the rotating board), the interface saves a "0" in the buffer. A parallel process is running in the microcontroller to send/receive data to/from the computer.
11. The microcontroller loops through the list until it receives a stop instruction from the computer.

The data acquisition computer and the USB interface are in a trailer about 100 ft away from the dynamo apparatus. To reduce the data transmission error caused by grounding, the signals between the USB interface and the stationary board are converted to differential voltage signals. On the stationary board, the differential address signal is converted to TTL signal by the line receiver to the rotating board; while the TTL data signal is converted to differential signal by the line driver to the USB interface. The line driver and line receiver are the only components on the stationary board relevant to the data acquisition in the rotating framework.

The software in the Linux-based data acquisition computer is written in C++. In the microcontroller, the firmware is in MPLAB C18 and MPASM Assembler.[15]

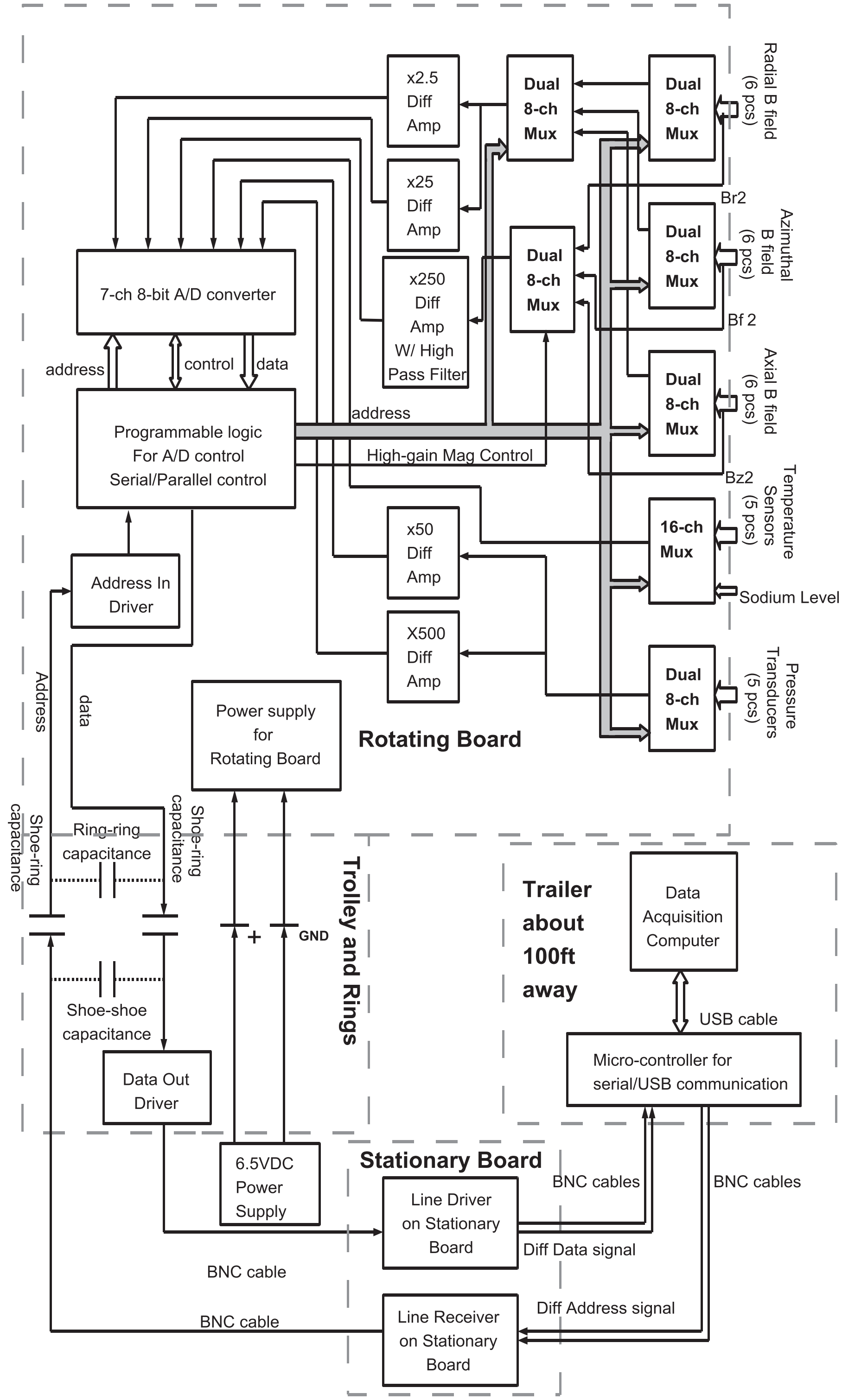

FIG. 2. The function blocks of the data acquisition system. On the rotating board, analog outputs of the sensors are digitized; parallel signals are converted to/from serial signals; serial address signals passed through the shoe/ring set are reshaped into TTL signals. Through the trolley/ring, DC power is supplied through brush/ring sets, serial address, and data signals are transmitted capacitively through shoe/ring sets. On the stationary board, serial signals are converted to/from differential signals. Differential signals are encoded/decoded by the microcontroller interface which communicates with the data acquisition computer via USB connection.

B. Data acquisition computer and USB interface microcontroller board

Modern operating systems in PCs, such as many Linux distributions, Windows, etc., can manage multiple tasks at the "same" time. However, most of them perform poorly on doing tasks "real time," e.g., in a fix time interval of 100 μs repeatedly. In contrast, a microcontroller-based circuit (like Microchip® 18F4550), though simpler in structure, dedicated to fewer tasks, can manage data sampling precisely

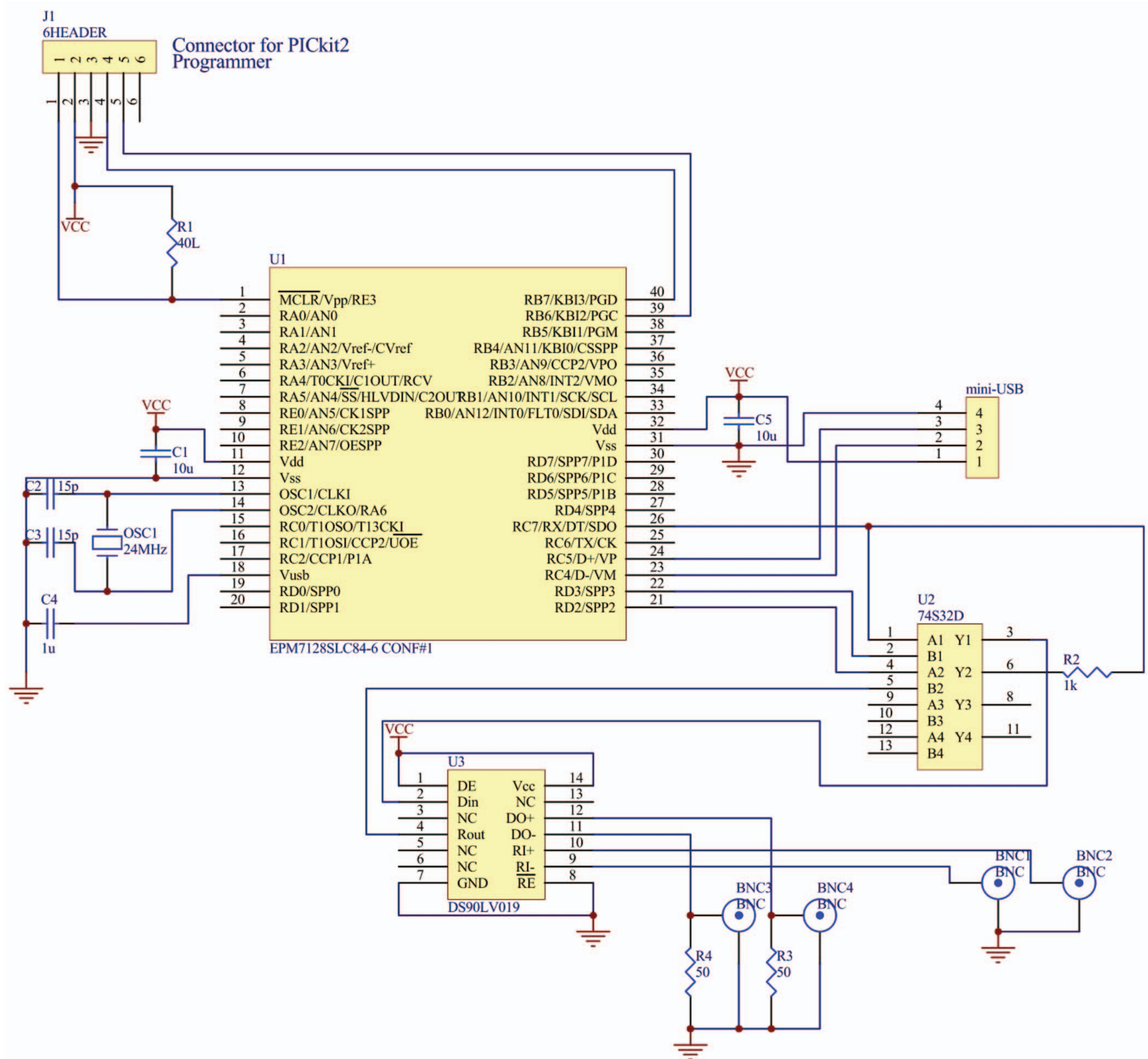

FIG. 3. The schematic of the USB microcontroller interface.

every 100 μs. In Fig. 3, U1 is the Microchip® 18F4550 microcontroller.[16] J1 is a connector for the Microchip® PICkit2/3 programmer/debugger. The microcontroller communicates with the computer through USB, and with the electronics on the dynamo apparatus through the Enhanced Universal Synchronous Asynchronous Receiver Transmitter (EUSART). The TTL signal levels from and to the microcontroller are converted to and from low voltage differential signal levels by a National Semiconductor® DS90LV019 line driver and receiver (U3). Two OR gates (U2, 74S32D) are used to switch between input mode and output mode (see Fig. 3).

Fig. 4 shows the simplified flow charts of the program in the computer and the microcontroller.

The tasks of the main process of the computer program are initializing the USB communication, handling the user input, creating Data Acquisition Thread (DAT), handling the data from the DAT, and instructing the DAT to terminate upon the user's request. For example, when we heat the apparatus up to 110 °C to melt the sodium, we start a mode to plot the timelines of the heating history from the temperature sensors. The main process generates a list of sensors according to the mode we input, then creates a new DAT thread running "in parallel" with the main process, passes the sensor list to the thread, indicates whether data should be stored in the hard drive. The main process continuously checks the shared buffer for any new data from the DAT thread. If so, the main process gets the data and handles it (e.g., plot it out). If user requests a stop, the main process sets the thread termination flag.

The DAT is created by the main process. It first instructs the USB interface when to start the data acquisition and which sensor(s) to query. The DAT continuously gets the data from

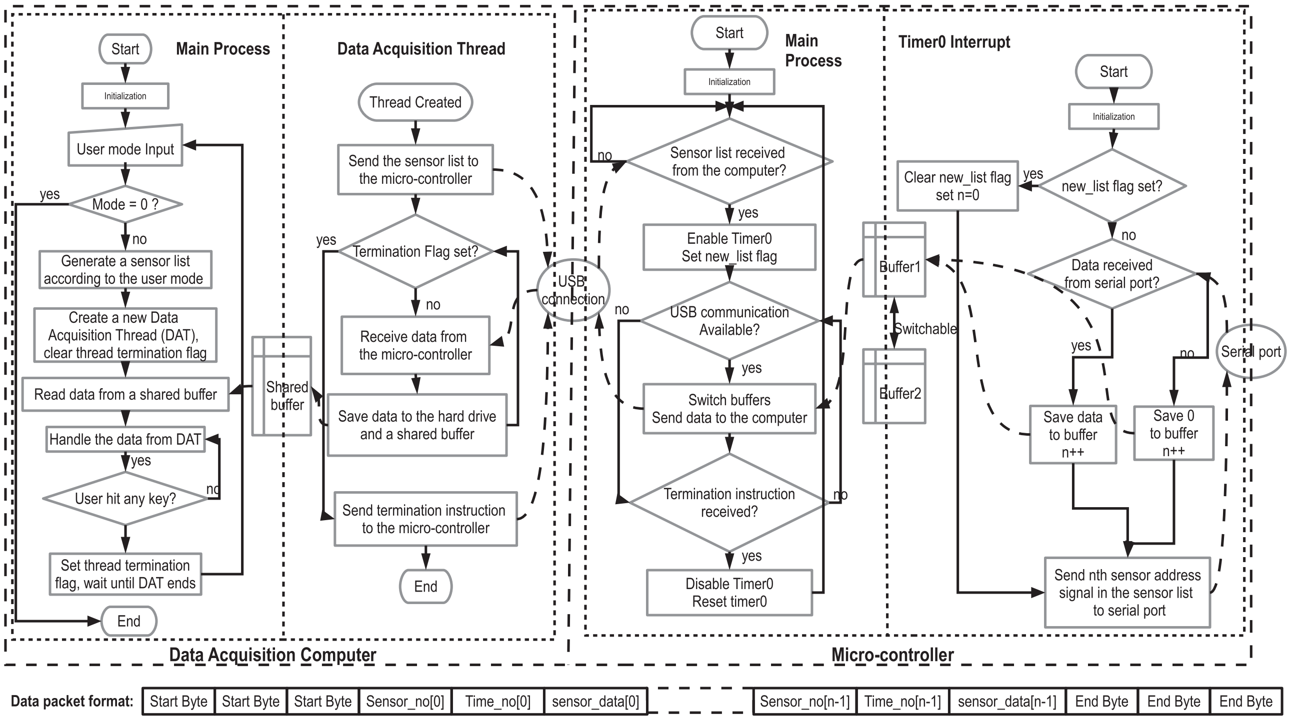

FIG. 4. Flow charts of the data acquisition softwares in the computer and microcontroller. From left to right are the main process of the data acquisition program and data acquisition thread in the computer, the main process, and timer0 interrupt in the microcontroller.

the USB interface, decodes it, saves it to a shared buffer and the hard drive (if required). When the thread termination flag is set, the USB interface stops data sampling.

When powered up, the microcontroller initializes the USB communication and EUSART function blocks, sets registers for data sampling, etc., then waits for computer instructions. Once instructions with a sensor list are received from the computer, the microcontroller enables one of its internal timers (timer0) which is triggered in every 100 μs and sets the timer0 interrupt priority as high. The interrupt handling thread sends out the serial address signals and receives the serial data signals. After enabling the timer0, the main microcontroller process continuously retrieves the data from the buffer shared with timer0 interrupts, sends the data to the computer, and checks whether there are new instructions from the computer. If a termination instruction is received, it stops data sampling by disabling timer0, then waits for the new instructions from the computer.

The sensor list from computer are numbers from 51 to 221. In the microcontroller, the sensor numbers are translated to 12-bit addresses which turn on the desired A/D converter and multiplexer channels. The data received from the electronics are 8-bit. When the microcontroller sends the data to the computer, to facilitate the error check, the data are grouped in packets with a format as shown in Fig. 4.

Although the flow charts are complicated, a user can simply type in a pre-defined mode number to instruct the computer to take data from a pre-defined list. To a user, a typical data acquisition procedure is as follows: the user starts the data acquisition program; types in a mode number, for instance, "47" to instruct computer to take data from sensors needed to plot the timelines of the heating history; the program then continuously plots the data in a window until an "enter" key is hit; the data acquisition program pauses and waits for the next mode number; the user can type in a "0" to quit the program.

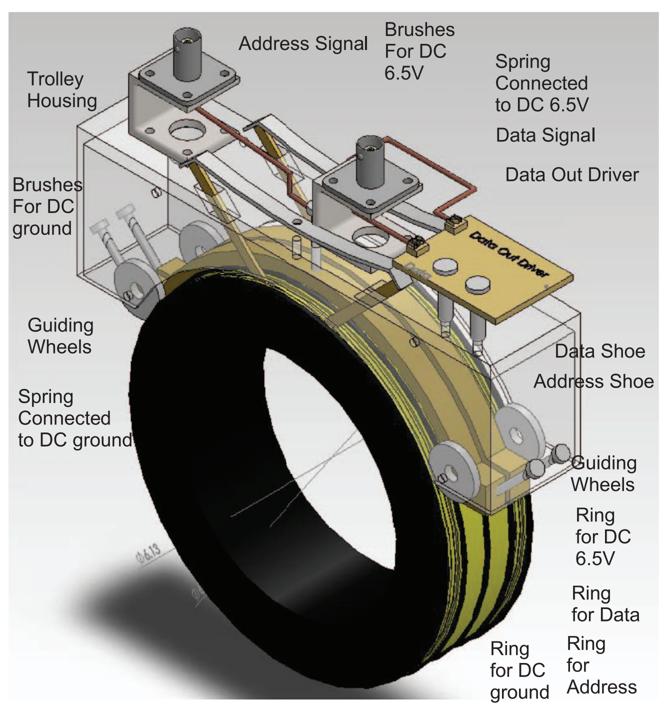

FIG. 5. Sketch of slip rings and trolley. The trolley housing has 4 brushes to provide DC power to the rotating board: 2 for ground and 2 for 6.5 VDC. The copper carbon brushes are held by springs. Address signals and data signals are transmitted through the gaps between the shoe/ring sets capacitively.

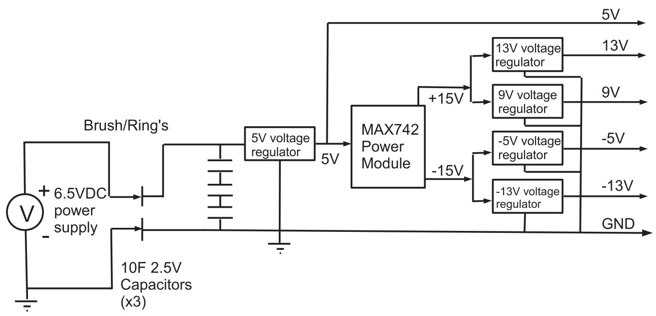

FIG. 6. The schematic of the power supply. A 6.5 VDC power is input through the brush/ring sets and converted to +5 V, −5 V, +9 V, −13 V, and +13 V powers on the rotating board.

The USB interface board is specified as a device of communications device class (CDC),[17] configured as an RS-232 emulator so that the computer can treat it a traditional RS-232 port with a proper device driver.

C. Slip rings and trolley

Fig. 5 is a drawing of the slip rings and trolley assembly. From left to right are the copper rings for DC power ground, address signal, data signal, and 6.5 VDC power, respectively. The leftmost and rightmost rings have tracks. The tracks guide 4 wheels supporting the trolley housing and keep the proper clearance (0.02 cm) between shoes and rings.

Two copper carbon brushes in contact with the ground and 6.5 VDC power rings are tensioned by a spring, on each side of the trolley. The address and data signal shoes are made of copper. The address signal and data signal are transmitted using BNC cables with the shield grounded. The address terminal is directly connected to the shoe. The data shoe is connected to the Data Out Driver. The DOD reshapes the data signal into standard TTL signal and transmits it to the stationary board.

The shoe-to-ring capacitances are determined by the clearance between the shoes and rings. We measured that the capacitances are around 125 pF at a clearance of 0.02 cm.

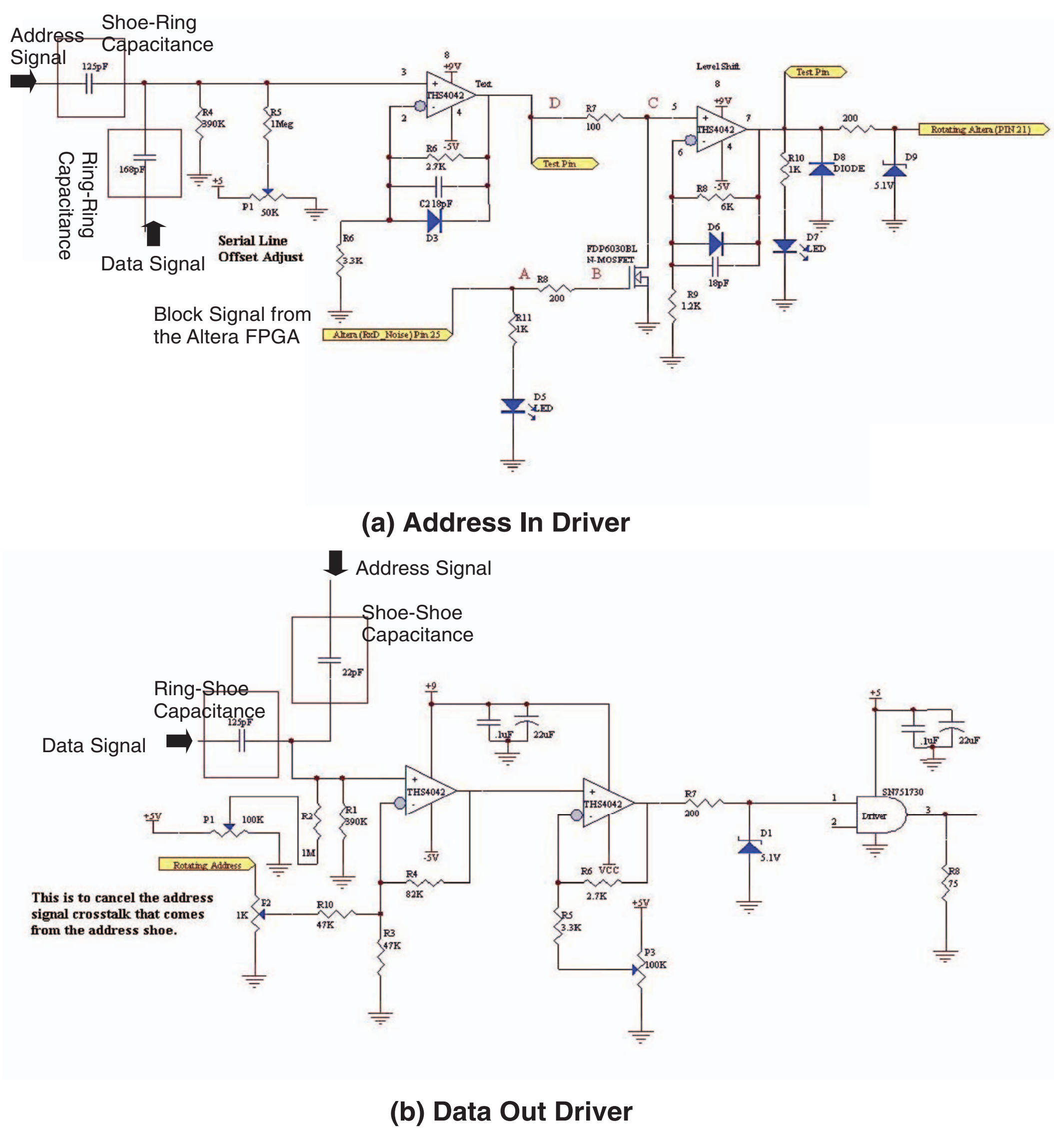

FIG. 7. (a) The Address In Driver (AID) on the rotating board. The AID reshapes the address signal coupled through the shoe/ring gap into TTL signal and blocks the cross-talk from the data ring to the address ring. (b) The Data Out Driver (DOD) on an independent board on the trolley. The DOD reshapes the data signal coupled through the ring/shoe gap into TTL signal and blocks the cross-talk from the address shoe to the data shoe.

The shoe-to-shoe capacitance is about 22 pF, while that of ring-to-ring is about 168 pF. The latter two values are comparable to the shoe-to-ring capacitances. While address signals can couple through the shoe-to-ring gap to the rotating board, they can also couple through the shoe-to-shoe gap, return to the computer, and make the computer treat them as data signals. Similarly, data signals can couple through the ring-to-ring gap to make the altera FPGA treat them as another incoming address signal. To prevent these from happening, we have to eliminate the cross-talks in the Address In and Data Out Drivers as described in Sec. II E.

D. Rotating board

The rotating board collects voltage signals from the sensors rotating with the dynamo outer cylinder as shown in Fig. 1(a), including 18 Honeywell® SS49E Hall sensors (6 sensors each for radial, azimuthal, and axial directions in a streamlined probe), 5 Honeywell® 13-series pressure transducers at 5 radial positions, 5 Analog Devices® TMP36 temperature sensors (2 on each of the two end-plates, 1 on the rotating board), and 1 circuit monitoring conductivity when liquid sodium fills between the cylinders.

As shown in Fig. 2, the signals are selected by multiplexers. To obtain enough resolution, amplifiers with different gains are used. A Maxim® MAX118 8-channel 8-bit analog-to-digital converter is used to convert the analog signal to digital signals. The multiplexers and ADC are controlled by an Altera® FPGA. The HDL codes in the FPGA are a variation based on the Universal Asynchronous Receiver/Transmitter (UART) technique.[18,19]

The components on the rotating board require different power supplies (VCC, GND, ±5 V, +9 V, and ±13 V). The schematic of the power supply is shown in Fig. 6. A 6.5 VDC power supply is used to power the rotating board through the brush/ring sets. To eliminate the ripples caused by the high speed spinning of the outer cylinder, high capacitance (10 F), low Equivalent Series Resistance ($<0.15\,\Omega$) (PowerStor® B1325-2R5106-R) electrolytic super capacitors are used. The rated voltage of the super capacitors is 2.5 V (which is the highest voltage available), so we used 3 of them in series. The input voltage is converted to 5 V using a 5 V voltage regulator (National Semiconductor® LM340T-5) for VCC power, +5 V analog power, and the input to a Maxim® MAX742 power module. The MAX742 module converts 5 V input into +15 V and −15 V power supplies. The +15 V power is converted to +13 V analog power by a Linear Technology® LT1085 voltage regulator, +9 V by a Fairchild Semiconductor® LM317T voltage regulator. Similarly, the −15 V power is converted to −13 V analog power by a Linear Technology® LT1175 regulator, −5 V by a Fairchild Semiconductor® LM7905.

The components on the rotating board are secured by epoxy to withstand the high-g centrifugal force. During the experiment, the board has refrigerated air flow to keep the components no higher than 30 °C. Teflon coated wires are used for connecting to the sensors. The wires and sensors are covered by silicone RTV for protection.

E. Address In and Data Out Drivers

The signal through the shoe/ring set is amplified by 2 stages of amplifiers in the Address In Driver (Fig. 7(a)). With the diodes D3 and D7, only the positive part of the signal is amplified. The shoe-ring set (with capacitance), R4, R5, and P1 form a first-order high-pass filter. The RC time is about 35μs, which is longer than the length of the serial address signal ($\approx 30\,\mu$s), so the address signal can pass through. The data signal sent back by the Altera® FPGA can couple through the ring-ring set. If there is no measure to suppress this cross-talk, the Altera® FPGA will "think" that this is another address signal. To suppress the cross-talk, during the period of data signal, the FPGA sends a high voltage "block" signal to a N-MOSFET (Fairchild Semiconductor® FDP6030) to lower the voltage at C in Fig. 7(a).

The stationary Data Out Driver in Fig. 7(b) is similar to the AID. A potentiometer is used as a voltage divider to feed some address signal back to the negative input of the amplifier to cancel the address signal cross-talk. We do not use this

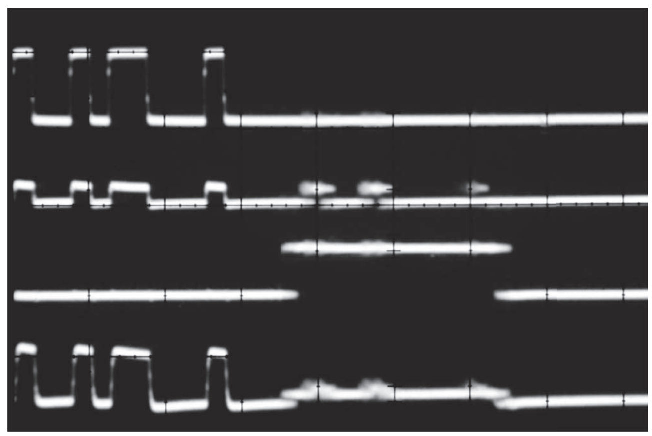

(a) Cross-talk Suppression by AID

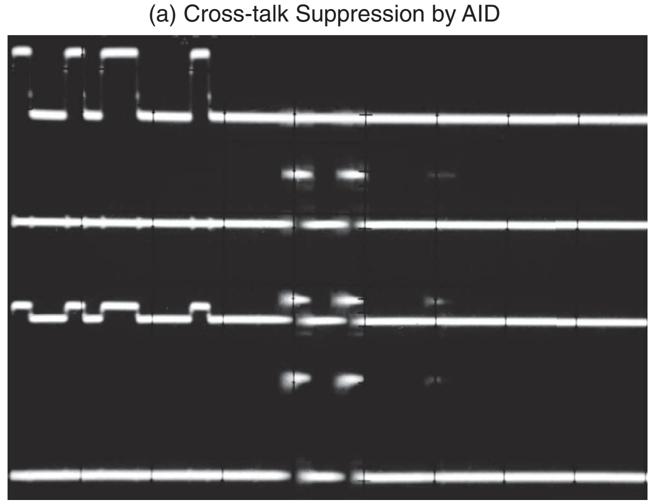

(b) Cross-talk Suppression by DOD

FIG. 8. Cross-talk suppression by the Address In and Data Out Drivers. In (a), from top to bottom are an address signal before the shoe/ring set, after the shoe/ring set with the data signal cross-talk, a "block" signal, and the signal to the Alter® FPGA with cross-talk suppressed, respectively. In (b), from top to bottom are an address signal, a data signal before ring/shoe set, and a signal after the ring/shoe set with the address signal cross-talk, and the reshaped signal by the Data Out Driver, respectively.

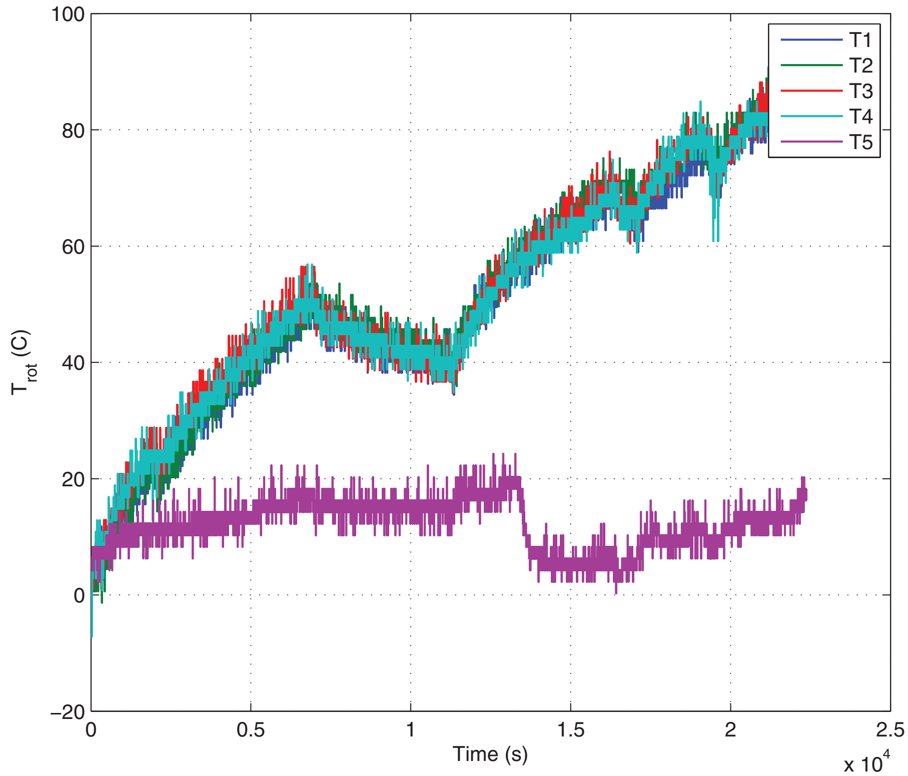

FIG. 9. The heating history on 2/16/2012. T1-T4 are the temperature sensors on the end-plates, T5 is the temperature sensor on the rotating board. The data rate is 1 sample per second for about 6.25 h.

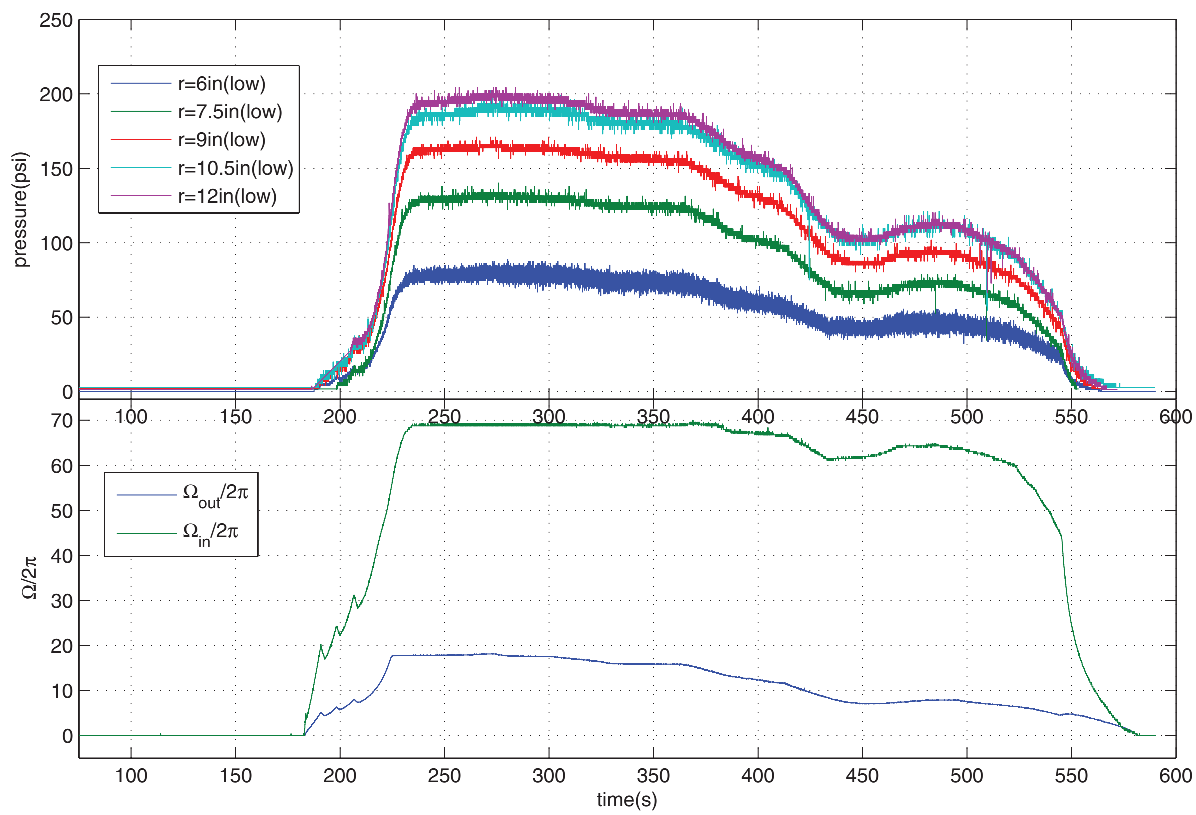

FIG. 10. Pressure vs time curve taken on 3/6/2012 with mineral oil at about 110 °C. The inner/outer cylinder speeds were up to $\Omega_{out} = 2\pi \times 17.6$ rad/s and $\Omega_{in} = 2\pi \times 68.9$ rad/s. The upper plot is pressures at 5 positions; the bottom plot is the rotation speed of the outer and inner cylinders.

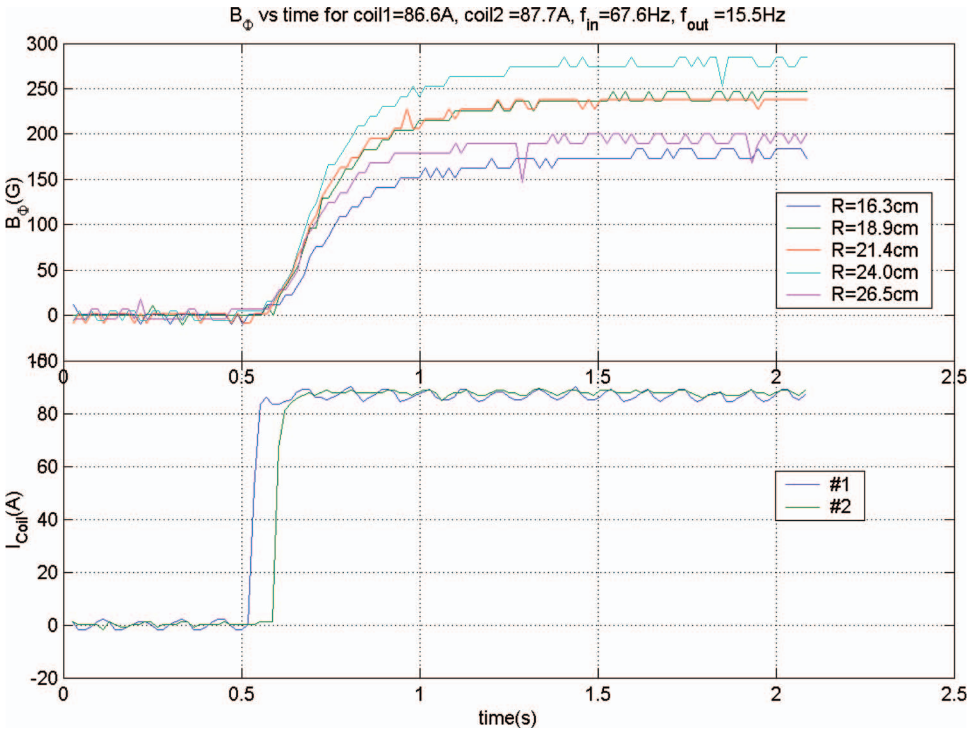

FIG. 11. The azimuthal magnetic field curves taken on 9/1/2009. The top plot is the azimuthal field B_ϕ at 16.3, 18.9, 21.4, 24.0, and 26.5 cm, respectively. The bottom plot is the current of coils #1 and #2. The dynamo apparatus is spinning at $\Omega_{in} = 2\pi \times 67.6$ rad/s and $\Omega_{out} = 2\pi \times 15.5$ rad/s with liquid sodium.

method on the AID because high speed spinning can stress potentiometers and cause them to change value.

III. SYSTEM TESTING

The data presented here are relatively "raw." The analysis of the physics can be found in PRL[20] (in which we have demonstrated experimentally a relatively large ω-gain $G_\omega \approx 8$).

Fig. 8(a) shows that the cross-talk is suppressed by the AID. As the address signal passes through the shoe/ring set, it is coupled by the data signal cross-talk through the ring/ring capacitance. With the "block" signal from the Altera® FPGA, this cross-talk is suppressed. Although not totally eliminated, it is low enough to make the Altera® FPGA treat it as "0." In Fig. 8(b), the address signal cross-talk is totally eliminated by the DOD.

Heating the apparatus is crucial for the experiment. Fig. 9 shows the heating history on 3/6/2012 over 6 h. T1-T4 show the temperatures on the end-plates, T5 the temperature of the rotating board. In the figure, T1-T4 varied by interruptions by other tests. We maintain the rotating board temperature below 30 °C with an air conditioner. Evaporator icing reduces air flow. This flow is restored by de-icing. In the figure, this appears as a sudden slump of T5 at about 1.3×10^4 s.

The pressure data in Fig. 10 were taken at a temperature of about 110 °C with mineral oil. When the apparatus first reached a stable state at about $T = 230$ s, the angular speed ratio was $\Omega_{in}/\Omega_{out} \sim 4 \sim R_{out}^2/R_{in}^2$, which is the marginal criteria for ideal stable Couette flows.[10] After the speed stabilized for about 50 s, we slowed the speed of the outer cylinder. Because the radial pressure gradient balances the centrifugal force, the pressure decreased with the speed of the outer cylinder. Note the inner cylinder speed at $T = 380$ s started to decrease, the ratio $\Omega_{in}/\Omega_{out} > 5$ already exceeded the threshold for Kelvin-Helmholtz stable. As the outer cylinder speed slowed, the flow became more turbulent, the angular momentum transported from the inner cylinder to the outer cylinder became larger, and the torque on the inner cylinder increased. Since higher torque requires more motor power, when the required power exceeded the motor capability, the motor could not keep the speed of the inner cylinder constant.

Fig. 11 shows an example of the azimuthal magnetic field measured on 9/1/2009 with liquid sodium in the dynamo apparatus and the inner and outer cylinder spinning at $\Omega_{in} = 2\pi \times 67.6$ rad/s and $\Omega_{out} = 2\pi \times 15.5$ rad/s. Driving the coils with DC currents in opposite directions generates a radial field. With the shear motion of the liquid sodium flow in the "seed" radial field, an azimuthal magnetic field results.

IV. CONCLUSION AND FUTURE PLAN

We have built a data acquisition system which can be used to retrieve data from sensors in a high-speed rotating frame at speed up to 17.5 revolutions/s and temperatures up to 130 °C. The data are digitized, converted to serial signals, and sent to a computer approximately 100 ft away. An FPGA and a microcontroller are used for the digitization. The system can withstand high temperatures and rotational speeds. Some of our experimental results have been published.[20]

As we plan for the α-phase, we are upgrading the data acquisition system by constructing an additional magnetic probe and a new rotating board with more ports.

Because current data sampling rate is limited by the processing ability of Microchip® 18F4550 microcontroller, we plan to upgrade to a more powerful microcontroller, Microchip® PIC32MX230F064D.

ACKNOWLEDGMENTS

We gratefully acknowledge the funding over the years by NSF, LANL via a cooperative arrangement with NMIMT, and the IGPP program at LANL. Many undergraduate students have participated in this project. NMIMT, EMRTC, CMSO, and many others have made this project possible. S.C. and H.L. also acknowledge the support by the LANL/LDRD program and the DoE/OFES via Center for Magnetic Self-Organization.

[1]S. A. Colgate, H. Li, and V. Pariev, Phys. Plasmas **8**, 2425 (2001).
[2]H. K. Moffat, *Magnetic Field Generation in Electrically Conducting Fluids* (Cambridge University Press, 1978).
[3]J. Larmor, Rep. Brit. Assoc. Adv. Sci. **47**, 159 (1919).
[4]E. N. Parker, *Cosmical Magnetic Fields: Their Origin and Their Activity* (Clarendon, Oxford, 1979).
[5]Y. K. Zeldovich, A. A. Ruzmaikin, and D. D. Sokoloff, *Magnetic Fields in Astrophysics* (Gordon and Breach, Science Publishers, 1983).
[6]See http://perso.ens-lyon.fr/nicolas.plihon/VKS/index.php?page=accueil, http://complex.umd.edu/research/MHD_dynamos/3m.php, and http://plasma.physics.wisc.edu/mde, respectively, for some of the dynamo experiments.
[7]S. M. Tobias and F. Cattaneo, Phys. Rev. Lett. **101**, 125003 (2008).
[8]V. I. Pariev and S. A. Colgate, Astrophys. J. **658**, 114 (2007).
[9]V. I. Pariev, S. A. Colgate, and J. M. Finn, Astrophys. J. **658**, 129 (2007).
[10]S. Chandrasekhar, *Hydrodynamic and Hydromagnetic Stability* (Dover Publication, Inc., New York, 1981).
[11]H. F. Beckley, "Measurement of annular Couette flow stability at the fluid Reynolds number Re $= 6 \times 10^6$: the fluid dynamic precursor to a liquid sodium $\alpha\omega$ dynamo," Ph.D. thesis (New Mexico Institute of Mining and Technology, 2002).
[12]H. F. Beckley, S. A. Colgate, V. D. Romero, and R. Ferrel, Astrophys. J. **599**, 702 (2003).
[13]F. Stefani, T. Gundrum, G. Gerbeth, G. Rdiger, J. Szklarski, and R. Hollerbach, New J. Phys. **9**, 295 (2007).
[14]E. Schartman, H. Ji, and M. J. Burin, Rev. Sci. Instrum. **80**, 024501 (2009).
[15]These compilers can be downloaded/purchased at http://www.microchip.com/.
[16]The datasheet of 18F4550 can be found at http://www.microchip.com/.
[17]The USB class specification documents can be found at http://www.usb.org/developers/devclass_docs.
[18]F. A. Scarpino, *VHDL and AHDL Digital System Implementation* (Prentice-Hall PTR, 1998).
[19]P. P. Chu, *FPGA Prototyping by VHDL Examples: Xilinx Spartan-3 Version* (John Wiley & Sons, Inc., Hoboken, New Jersey, 2008).
[20]S. A. Colgate, H. Beckley, J. Si, J. Martinic, D. Westpfahl, J. Slutz, C. Westrom, B. Klein, P. Schendel, C. Scharle, T. McKinney, R. Ginanni, I. Bentley, T. Mickey, R. Ferrel, H. Li, V. Pariev, and J. Finn, Phys. Rev. Lett. **106**, 175003 (2011).